SCIENCE CHINA
Physics, Mechanics & Astronomy

•Invited Review•

June 2022 Vol. 65 No. 6: 264601
https://doi.org/10.1007/s11433-021-1853-3

Molecular transport under extreme confinement

FengChao Wang, JianHao Qian, JingCun Fan, JinChuan Li, HengYu Xu, and HengAn Wu*

CAS Key Laboratory of Mechanical Behavior and Design of Materials, Department of Modern Mechanics, CAS Center for Excellence in Complex System Mechanics, University of Science and Technology of China, Hefei 230027, China

Received November 25, 2021; accepted January 7, 2022; published online April 25, 2022

Mass transport through the nanoporous medium is ubiquitous in nature and industry. Unlike the macroscale transport phenomena which have been well understood by the theory of continuum mechanics, the relevant physics and mechanics on the nanoscale transport still remain mysterious. Recent developments in fabrication of slit-like nanocapillaries with precise dimensions and atomically smooth surfaces have promoted the fundamental research on the molecular transport under extreme confinement. In this review, we summarized the contemporary progress in the study of confined molecular transport of water, ions and gases, based on both experiments and molecular dynamics simulations. The liquid exhibits a pronounced layered structure that extends over several intermolecular distances from the solid surface, which has a substantial influence on static properties and transport behaviors under confinement. Latest studies have also shown that those molecular details could provide some new understanding on the century-old classical theory in this field.

confined mass transport, nanocapillary, solid-liquid interface, confinement effect

PACS number(s): 34.20.Gj, 61.20.Ja, 62.10.+s

Citation: F. C. Wang, J. H. Qian, J. C. Fan, J. C. Li, H. Y. Xu, and H. A. Wu, Molecular transport under extreme confinement, Sci. China-Phys. Mech. Astron. **65**, 264601 (2022), https://doi.org/10.1007/s11433-021-1853-3

1 Introduction

Human's interest in the transport of water has tremendous effects on the development of civilization [1,2]. The famous Roman aqueduct was built more than 2300 years ago, but its history may date back to the 7th century BC, when the Assyrians built an 80 km long limestone aqueduct to carry water to their capital city, Nineveh [3]. From the perspective of scientific research, the pioneers of hydrodynamics, whose preeminent names include but not limited to Euler, Bernoulli, Navier, Stokes, and Reynolds, established the fundamental theory of fluid motion [4]. Thereafter, the blooming exploration on the liquid flow and related transport brings great vitality to this field. With the emergence of micro-electro-mechanical systems and microfluidic-based lab-on-the-chip, which began in the late 1980s, the characteristic dimension of research concerns is continuously decreasing, even down to nanometer scales [5]. In most recent years, there are significant achievements which promote the remarkable progress of nanofluidics [6,7]. Here we would like to quote the title of a Comment published in *Nature Materials* by Lydéric Bocquet—"*Nanofluidics coming of age*" [8].

With the reduction in channel size, the opposite solid-liquid interfaces start to overlap, imposing an essential influence on the structure, interactions and properties of the liquid [9]. The terminology of confined liquids has been used for more than 30 years, when surface force apparatus made substantial contributions on this topic [10,11]. Under extreme confinement, the liquid can no longer be considered as a structureless continuum, which leads to an oscillating structural force when two solid walls approach [12].

Prior to the discussion on its dynamic transport, here it

*Corresponding author (email: wuha@ustc.edu.cn)

should be first emphasized that water under extreme confinement exhibits abnormal structural features compared with its bulk counterpart. A single-file water chain can be found in a carbon nanotube (CNT) with a diameter of sub-nanometer [13,14]. While in the two-dimensional (2D) capillaries, the confined water exhibits a pronounced layered structure that extends over several intermolecular distances from the surface [15]. The water density peaks gradually decay and eventually converge to the bulk value, as shown in Figure 1(a). In addition, shown in Figure 1(b), the hydration shells formed around dissolved ions present a somewhat analogous structure [16], if the ion is treated as the smallest solid element. On the other hand, the confinement effect would cause the rearrangement of hydrogen bond network of 2D water along the direction parallel to slit walls. A quadrilateral structure can be found within the confined space which only accommodates the monolayer water [17]. Although there are some controversies, especially on the experiments [18], a large amount of computer simulations have confirmed this quadrilateral structure [19-21]. Moreover, such a special structure would result in unexpected low interfacial friction [21], as shown in Figure 1(c).

Structure determines properties. It has been widely reported that some transport properties of confined liquids demonstrate significant deviations from the bulk values [6-9], including diffusion coefficient, shear viscosity and thermal conductivity. Besides, anomalously low dielectric constant of confined water has been demonstrated in experiments and it exhibits a strong size dependence on the channel size [22]. These properties act as basic parameters in the governing equations. Consequently, it is inappropriate to employ the classical continuum theory, together with the macroscopic parameters, to describe the transport behaviors under extreme confinement [7]. There is therefore an urgent need for novel insights into the mechanisms of molecular transport at the nanoscale, a fresh understanding of these basic parameters, and the necessary corrections to the fundamental equations which are supposed to be valid only on the macroscale.

Categorized by different substances, the molecular transport of water, ions, gas and oil has attracted broad research interest from the academic communities. All of them have well-defined and substantial application prospects. For example, well-controlled nanometric-size containers for water and other solvents provide the environment and preconditions for "nanoconfined chemistry" [23]. Permeation and sieving of hydrated ions through nanochannels act as a research prototype in membrane science, which may disclose various fascinating aspects, like separation, distillation, osmosis, and desalination [24,25]. The transport of oil and gas through a nanoporous medium has also received plenty of attention, because of the important application background in the unconventional oil and gas development [26,27]. Even though the gas in confined space may not exhibit a distinct layered structure as the liquid does, the interfacial effect still plays an important role in gas transport [28], as shown in Figure 1(d). In particular, shale oil, as the name implies, is an unconventional oil produced from oil shale rock fragments by pyrolysis, hydrogenation, or thermal dissolution. Generally, the classical Darcy's law is not capable of accurately describing the transport behavior of oil and gas in shale reservoirs with abundant nanopores, exhibiting very low permeability [26,27]. On August 25, 2021, the discovery of a major shale oilfield in Daqing was announced, and added 1.268 billion tonnes worth of geological reserves from the Gulong formation. The mechanism of solid-liquid-gas interactions and enhanced oil recovery has been proposed as one of the six key scientific problems in the production of Gulong shale oil in the Songliao Basin [29]. The thorough investigation and in-depth understanding on the oil and gas

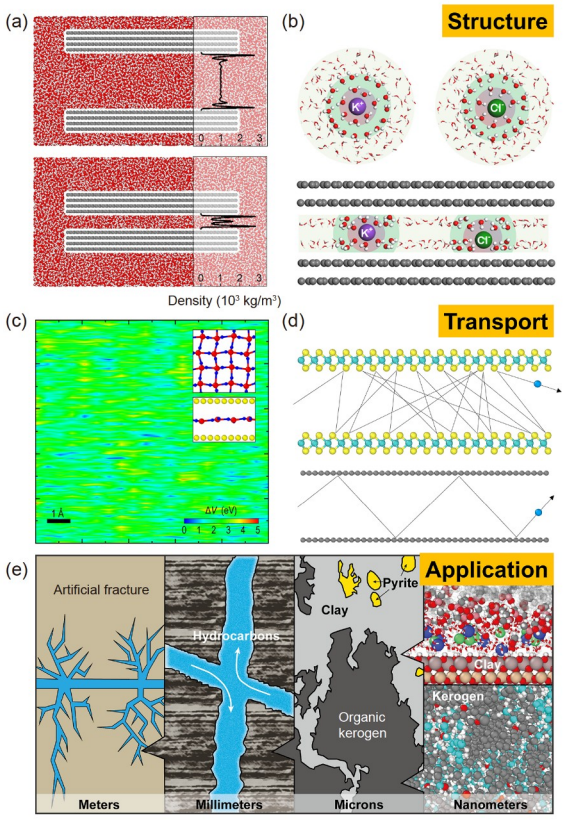

Figure 1 (Color online) Illustrations of structure, transport and application of molecular transport under confinement. (a) Layered structure of confined water extends over several intermolecular distances from the solid surfaces and these opposite structures start to overlap under extreme confinement. (b) Schematics of hydrated K^+ and Cl^- ions in bulk solutions and inside a channel of 6.8 Å in height. The first and second hydration shells are represented with pink and green shadows, respectively. Reprinted with permission from ref. [16]. Copyright©2019 American Chemical Society. (c) Potential energy surface of confined monolayer water with a quadrilateral structure (inset), which indicates an anomalously low friction. (d) Gas transport through nanochannels with diffuse (top) and specular (bottom) scattering. (e) Schematic diagram of the shale oil development as a multiscale problem.

transport in nanopores will play a pivotal role in the successful development of Gulong shale oil [29], as illustrated in Figure 1(e).

In this review, we put the spotlight on very recent insights into the molecular transport through nanochannels. Due to the limited space of the present paper, we mainly focus on the transport behaviors of water, ions and gases inside slit-like nanocapillaries. For a comprehensive knowledge of this flourishing field, we recommend readers refer to other reviews [6-9,24,25,30,31].

2 State of the art in experimental investigation

With the urgent demand for the understanding of molecular transport on such a small scale, experimental observations have been conducted on various platforms, such as CNTs [13], laminar graphene oxide (GO) membranes [32-34], nanopores in natural porous materials such as metal-organic frameworks (MOFs) and covalent organic frameworks (COFs) [35], or artificial nanochannel devices [31]. Despite many impressive achievements, there are two main types of disadvantages inherent in these nanopores for the study of confined mass transport. First, accurate control on the size of nanochannels is still challenging. It is expected that the measured flow rate through nanochannels can be compared and analyzed with predictions of theoretical models, which requires precise dimensions and geometries to implement the calculation. Second, the conventional materials and fabrication techniques limit the improvement to control the surface roughness and surface charge. The boundary conditions become increasingly crucial for the nanoscale flow. In some cases, the surface roughness is on the same order of the channel size.

More recently, a novel design of nanocapillaries to solve the two aforementioned issues has become feasible at the University of Manchester, which was referred to as van der Waals (vdW) assembly [36-39]. Here is the brief procedure of the fabrication, which was also sketched in Figure 2. First, a crystal of layered material, which is referred to as the bottom layer and specifically could be either graphite, hexagonal boron nitride (hBN), molybdenum disulphide (MoS_2) or mica, was transferred onto a silicon nitride (SiN) membrane with a rectangular hole, as shown in Figure 2(a). This hole in the SiN membrane was prepared in advance and can be used as a mask of the dry etching to the bottom layer. Then, a spacer with a certain height (different layers of 2D materials) was exfoliated onto an oxidized Si wafer and patterned using electron beam lithography and dry etching. The spacer array was subsequently transferred onto the bottom layer, aligning the stripes perpendicular to the long-axis of the rectangular hole, shown in Figure 2(b). The resulting stack was again dry etched from the backside to remove the spacer stripes from inside the hole. Then, another thin crystal (referred to as the top layer) was transferred on top of the stack, providing the enclosure of slits, as shown in Figure 2(c). This procedure can also be analogous to building with Lego, but on the atomic scale [40], as illustrated in Figure 2(d)-(f). The schematic of the experimental device is given in Figure 2(g) and the resulting nanocapillaries are shown in Figure 2(h) and (i). This approach generates nanochannels with precisely defined geometry. Here, the height of such nanocapillaries is determined by the thickness of the spacer. For instance, a monolayer graphene as the spacer leads to the extreme height of 3.4 Å [39] while the bilayer graphene determines the height to be about 6.7 Å [37]. The width of each channel is on the order of 100 nm. The channel length can be controlled by dry etching on a gold strip placed on the top crystal, usually several microns [37].

Such confined space for molecular transport can be viewed as one or several layers of 2D materials extracted from the bulk crystal. As we all have known, the monolayer graphene was isolated in a similar way, leading to the Nobel Prize in Physics in 2010. The left cavity is referred to as 2D empty space [41], or 2D nothing, which is the focus of the present review. Intriguingly, the contemplation on graphene and 2D empty space reminds us of a very famous saying in traditional Chinese philosophy “Being and non-being interdepend in growth”, which comes from Lao-Tzu’s *Tao Te Ching*. The graphene acts as a high-performance carrier for electronic transport and it displays remarkable electron mobility at room temperature, with reported values in excess of 150000 $cm^2\ V^{-1}\ s^{-1}$ [41]. Electrons in encapsulated graphene

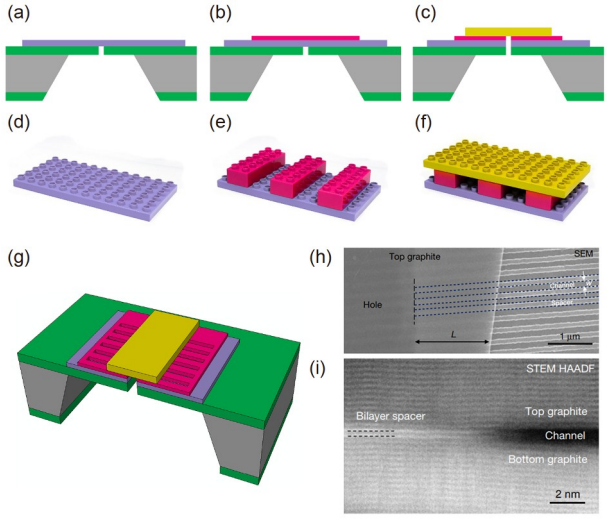

Figure 2 (Color online) (a)-(c) Illustrations of the microfabrication process of vdW assembled nanocapillaries; (d)-(f) analogy to atomic-scale Lego resembles; (g) schematic of the devices; (h) scanning electron microscopy (SEM) image of a trilayer device (top view); (i) high-angle annular dark field (HAADF) image of the edge of a nanocapillary with bilayer graphene as the spacer; (h), (i) adapted with permission from ref. [36]. Copyright©2016 Springer Nature.

exhibit exotic hydrodynamic effects, which can be described by the Navier-Stokes equations [42]. On the other side of the coin, 2D empty space brings us new insights for confined mass transport, in which the velocity of water can reach up to 1 m/s [36] and the helium gas flow is of orders of magnitude faster than the expected value from the Knudsen theory [38].

3 Molecular transport under confinement

With those designed nanocapillaries with precise dimensions and atomically smooth surfaces, one can investigate the transport behavior of various substances, including water, ions, and gas, which will be discussed sequentially in the following subsections. The determined geometry of nanocapillaries allows us to compare the transport flux measured in experiments with the prediction from a classical theory, to evaluate whether the theory is valid on the nanoscale. In addition, recent experiments have reported various unexpected results under extreme confinement, which expands our knowledge and improves our understanding on the molecular transport.

3.1 Water transport

Under extreme confinement, water transport usually exhibits extraordinary behaviors. Exceptionally fast water permeation through a network of nanocapillaries formed within GO membranes was reported by Nair et al. [32] in 2012. Meanwhile, the diffusion of many other small-molecule gases, including helium whose molecular size is even smaller, is prevented in these GO laminates [32]. The unimpeded water transport was interpreted by the combined role of the capillary-like pressure due to the surface evaporation and the near-frictionless motion of monolayer water with a quadrilateral structure [32]. Experiments on the pressure-driven water flow rate through individual CNTs show distinct radius-dependent features. The estimated slip length can be 300 nm for CNTs with a radius of 15 nm. In contrast, no slippage in boron nitride nanotubes was observed, probably due to the different electronic properties [43].

Unexpectedly fast water flow was also observed in slit-like 2D nanochannels [36], while the large slip length of water over graphene surfaces (about 60 nm) is just one of the explanations. There is a non-monotonic relationship between the water flux Q and the capillary height h, as shown in Figure 3(a). Only when $h > 2$ nm, Q approximately increases linearly with h, as expected from the solution of a planar Poiseuille flow, if we simply considered the pressure due to a curved meniscus, $P = 2\gamma\cos\theta/h$. For $h < 2$ nm, Q manifests an unanticipated deviation from the linear dependence on h, which is attributed to the contribution of disjoining pressure to the capillary pressure. The disjoining pressure originates from water-surface interactions. It might reach up to 1000 bar (1 bar=10^5 Pa) and becomes dominant at the nanoscale, but

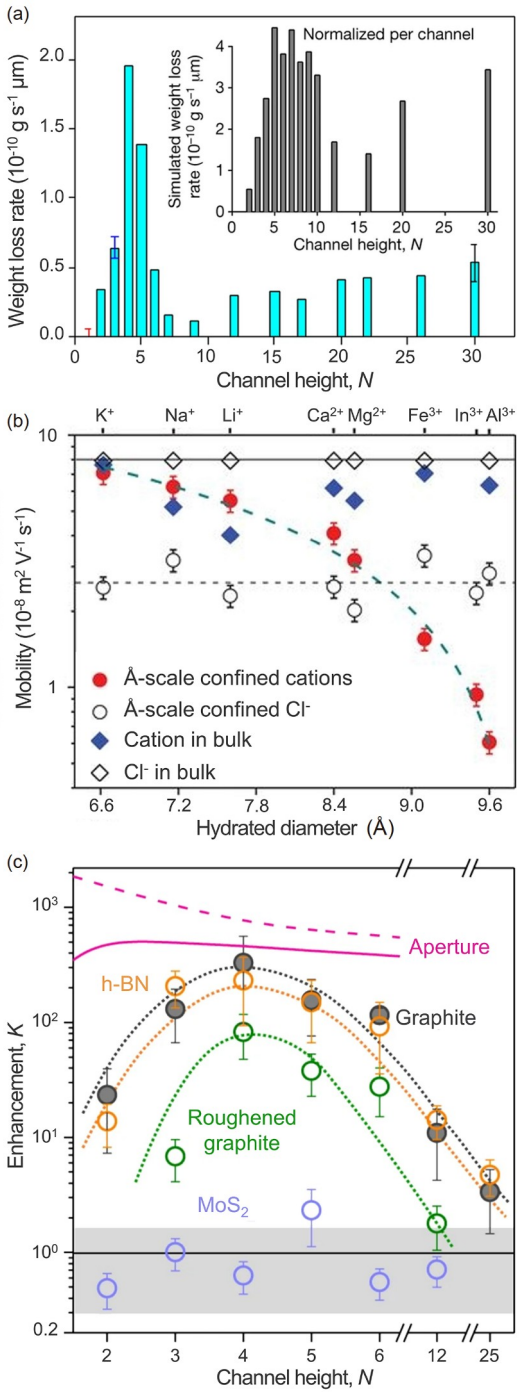

Figure 3 (Color online) Size effect on molecular transport under confinement. (a) Dependence of water flux through slit-like 2D nanochannels on capillary height. Inset, results found in molecular dynamics simulations. Reproduced with permission from ref. [36]. Copyright©2016 Springer Nature. (b) Ion mobility under the confinement as a function of the hydrated diameter [37]. Reprinted with permission from AAAS. (c) The observed enhancement of gas flux through nanocapillaries with respect to Knudsen theory for different channel heights and wall materials. Adapted with permission from ref. [38]. Copyright©2018 Springer Nature.

rapidly decreases with increasing h [36].

3.2 Ion transport

Once ions are dissolved in aqueous solutions, they attract and hold some water molecules, forming several concentric hydration shells. The diameter of hydrated ions ranges from a few angstroms to more than 1 nm, dependent on the attractive forces between the anion or cation and the surrounding water molecules. When those hydrated ions pass through the vdW assembled nanocapillaries, the size effect of transport behaviors or even the steric exclusion can be anticipated [37,39]. The hydration shells are flexible, allowing exchange of water molecules between the hydration shells and the surroundings, which brings more mystery.

Experiments reported that ions with hydrated diameters larger than the 2D slit's height (about 6.7 Å) can still permeate through, indicating an extrusion, deformation or even dehydration of the hydration shell [37]. The ion mobility, which is defined as the ratio of the drift velocity to the magnitude of the electric field, exhibits a clear reduction because of the confinement, as shown in Figure 3(b). There is also a notable asymmetry between anions and cations. The measured ion mobility of Cl^- decreases to nearly 1/3 of its bulk value, and it varies little for different salts under confinement. On the contrary, the ion mobility of cations decreases significantly with the increasing hydration diameters. In particular, the ion mobility of K^+ remains almost unchanged by the confinement, despite K^+ and Cl^- disclosing quite close hydration diameters and similar mobilities in bulk solutions [37].

From an intuitive perspective, the entire process of ion transport through these 2D angstrom-scale slits can be considered as three successive stages: entering the channel from the bulk phase, travelling inside the slits, and leaving the channel from the exit. The energy barriers required to accomplish the ion permeation are strongly dependent on the competitive relationship between the hydration diameter and the slit size [44]. As the slit size approaches the ultimate scale, dehydration at the entry impedes the ion transport remarkably, and even induces a complete ion rejection. When the height of nanocapillaries is reduced to 3.4 Å using the monolayer graphene as the spacer between top and bottom crystals, only water and proton can be permeated [39]. Experiments have reported that the diffusion constant of protons within the monolayer water is much lower than that through single-file water chain and that in the bulk water. This is not surprising since proton transport between water molecules should be understood from the Grotthuss mechanism. The ordered hydrogen bonding in 2D water should suppress rotation of water molecules with respect to 3D water, while the 1D hydrogen bonding in water chain can enhance proton diffusion [39].

3.3 Gas transport

The vdW assembled nanocapillaries were also implemented in the investigations on gas transport [38]. Unlike the situations discussed earlier, in which the structure of confined water and hydrated ions has an important impact on the transport dynamics, here more attention should be paid to the interface effect for gas transport [28]. In the regime of free molecular flow, the interactions among gas molecules are negligible and the gas-wall collisions are dominant.

Both experiments and simulations have shown that the helium gas flow rate through graphene or hBN nanochannels manifests an anomalous enhancement in comparison to the classical theory, while the gas flux through the atomically flat MoS_2 nanochannel can be generally described by the Knudsen equation [28,38]. The underlying mechanism was revealed as the surface morphological effect on the gas collision with solid walls. Even a subtle distinction of surface roughness results in specular scattering on graphene surfaces but diffuse scattering on MoS_2 surfaces [28]. At room temperature, the kinetic diameter and de Broglie wavelength of helium are approximately 2.6 and 0.5 Å, respectively. The equipotential surface of MoS_2 exhibits stronger corrugations than that of graphene and hBN. Thus helium can feel a smoother surface of graphene and hBN, resulting in more specular reflection [38].

More intriguingly, experiments on hydrogen and deuterium permeation have indicated the quantum effect on the gas transport. Hydrogen and deuterium have the same kinetic diameter and the same interaction with the walls but different de Broglie wavelength. However, the flow rate of deuterium through a graphene nanochannel is 30% ± 10% smaller than that of hydrogen, which is inconsistent with the prediction from the Knudsen equation, suggesting that the heavier deuterium with a shorter de Broglie wavelength sees an atomic landscape that is rougher than that seen by hydrogen [38].

4 Molecular dynamics simulations

Molecular dynamics (MD) simulations have played an important role in studying the transport process for the past several decades [5,7,23,24]. At the beginning, MD simulations only focus on the channels with characteristic dimensions of a few nanometers, because of the limits of computing power. Thus there is a size gap between simulations and experiments at that time. As supercomputer capabilities continue to grow and experimental techniques are constantly improving, now it becomes realistic for MD simulations to model the nanochannels having the same size as that employed in experiments [36,44], especially for the aforementioned vdW assembled capillaries, which may lead

to direct comparisons between simulations and experiments. Currently, classical MD simulations are capable of dealing with models tens of nanometers in height and one hundred nanometers in width. In general, channel lengths can also be in the tens of nanometers, hundreds of nanometers and even in the micron range for gas transport [28]. In some special cases, if periodic boundary conditions are used, the limitation on the length of the channel can be disregarded.

4.1 New insight from MD simulations

When a dynamic process is scrutinized, it is inevitable to discuss different kinds of driving forces in the first place. For ions in the aqueous solution, applied electric field or concentration gradient can be implemented to generate the ion migration, no matter how small the pore is [37]. However, the traditional pressure drop is not practical to drive the liquid flow through nanochannels because it is laborious to integrate supplemental pumping components with nanocapillaries. In recent years, evaporation has been used to drive water transport under extreme confinement [45]. The evaporation results in a low density region at the channel outlet, which further applies a drag on the liquid inside the nanochannels. Thus the liquid flow flux through nanochannels is identical to the evaporation flux. Then the drag action can be estimated as the effective pressure gradient applied on the liquid flow, which builds a connection between the two stages. Investigations based on MD simulations were carried out to evaluate the liquid flow through nanochannels driven by evaporation at the outlet [45]. MD results have shown that the pressure gradient is not constant at a given temperature and relative humidity, but exhibits a clear dependence on the channel length. This is because the total energy dissipation of liquid flow through nanochannels during evaporation is length-dependent. MD simulations found that lyophilic channels show higher evaporation fluxes than lyophobic channels. Moreover, the local evaporation flux from the solid-liquid interface is higher than that from the liquid-vapor interface at the middle region of the channel, which could explain why experimentally observed evaporation flux through nanochannels could exceed the limits predicted by the classical Hertz-Knudsen equation. These findings also help to understand the permeance of engineered COF-based membranes used for membrane distillation [35].

Evaporation-driven water transport through 2D slits shows a striking enhancement in flow rate as $h < 2$ nm. This was elucidated by introducing the concept of the disjoining pressure [36]. MD simulations confirmed that when the channel height is less than 2 nm, the pressure applied on the confined water increases particularly faster than the classical estimation considering the curved meniscus [36,46]. The disjoining pressure consists of several contributions, including the vdW interactions, the electrostatic component and the entropic term due to the liquid structuring under confinement. The slip length of water flow on graphene is not sufficient to interpret the notable enhancement of water flow rate observed in experiments. With the simulated pressure, the experimental findings can be qualitatively reproduced [36]. Based on these understandings, we think the enhancement of water flow rate widely reported in ref. [36] can be well described if the appropriate driving force and slip length are taken into account when applying theoretical formulas. MD simulations have made some progress on this topic, but there are still many questions that deserve further research.

MD simulations also provided new insights into the molecular-scale details regarding structures and dynamic processes of ion transport [16,24,44,47]. One of the basic principles involved is size exclusion, in which the ion transport is modulated by the competition between diameters of hydrated ions and channel sizes. The hydration layers formed around dissolved ions are analogous to ordered structures of water in the vicinity of a solid surface. There is a balance of configurational competition between the bilayer water under confinement in a channel with height of 6.7 Å and the concentric hydration shell [24]. Cl^- ions would rather to locate in either one of these two water layers, closer to the graphene walls, while K^+ ions have a concentrated distribution between two layers. Opposite charge leads to dissimilar water dipolar orientations around ions, mediating the distance and tribological interactions between hydrated ions and walls. Consequently, hydrated Cl^- ions encounter a remarkably larger friction force inside the channel and thus manifest a smaller mobility compared with K^+ ions, which is consistent with the charge asymmetry effect on ion mobilities reported in experiments [37].

The extraordinary layered structure of water at the solid-liquid interfaces is not considered in the framework of continuum theory. It can, however, have a non-negligible impact on the macroscopic thermodynamic properties. Here is an example about the solid-liquid interface energy [15]. Let us image two rigid solid walls immersed in a water box which is large enough to allow water molecules confined between two solid walls to exchange easily with outside molecules. If the initial spacing is large enough, it can be anticipated that the opposite walls would not “feel” each other, and the layered water structures near surfaces remain undisturbed in reference to the case of infinite spacing. Then the two solid walls are brought progressively closer at a slow speed. Once the walls are in a sufficiently short distance, the layered structures overlap, and extra work is required to rearrange water molecules into the intensely layered structures. MD simulations demonstrate that the potential energy of the entire system exhibits pronounced oscillations. Such variation can be attributed to the deviations in the solid-liquid surface energy from the bulk value, since there are no other sig-

nificant changes to the system. As a consequence, when applying the macroscopic Kelvin equation to characterize the condensation transition under atomic-scale confinement, the size effect of solid-liquid interface energy should be considered [15]. In addition, if the two confining walls are not completely rigid, which is more realistic under practical circumstances, the contribution from elastic adjustments of solid walls to the variation of solid-liquid interface energy should be taken into account.

The gas flow through nanochannels can be quantitatively described by the Knudsen theory, which assumes the completely diffuse reflection of gas molecules on the confining walls. Experiments have revealed the possibility of specular reflection on some atomically smooth surfaces, eventuating in an abnormal enhancement of gas flux [37]. The surface morphological effect was proposed by MD simulations. A delicate difference in surface roughness leads to the diffuse scattering on MoS_2 surfaces while specular scattering on graphene surfaces. It was also found that the curvature effect could decrease the surface roughness of potential surfaces, leading to an extra enhancement on the gas flow rate [28].

4.2 Limitations of MD simulations

Although MD simulations have demonstrated a strong ability to provide atomic-scale detail in this field, modeling and simulations can never substitute for real-world experimentation. One should keep in mind that MD simulations still have some intrinsic limitations and that extra care should be taken when analyzing the simulation results.

The accuracy and adaptability of empirical potential functions and parameters employed in classical MD simulations have been a long-standing criticism. For example, there are dozens of water models that have been widely used in MD simulations [48]. All these popular water models were developed to reproduce the bulk properties of water, such as density, diffusion coefficient, surface tension, and heat capacity. When our focus turns to water under confinement, it can be expected that those non-polarizable models may not be able to accurately describe the static and dynamic behaviors of the confined water. Recently, researchers start to develop more accurate water models based on the artificial intelligence/machine learning (AI/ML) algorithms [49-51], which could probably offer us a solution to this issue. In addition, similar limitations also exist in the potential models for ions, gases and solid walls. We anticipate that the future force field can take into account of the influence of fluid-solid coupling and solvent effect on the dissolutive flow [52,53].

For water, it is still difficult to simulate its phase change process under ambient conditions in MD simulations, because a prohibitively large simulation box is required due to the low density of water vapor [36]. In most MD simulations, only a simplified model of water flow in a nanochannel is considered, while the evaporation or condensation as an additional entrance effect is usually disregarded. This concession sacrifices some key elements in the big picture of molecular transport. Additionally, even though some properties can be calculated from MD simulations based on the statistical-mechanical theory, such as viscosity and pressure, their significance at the nanoscale deserves further speculation. For example, viscosity is a continuum quantity, without considering the liquid structure from a nanoscale perspective. Thus it would lose its fundamental meaning and might bring in notable error in the estimation on the water flux under confinement.

5 Theory: Solid-liquid interface mechanics

There is already a consensus that molecular transport under extreme confinement can not be precisely described by the classical mechanical theories derived on the basis of the continuum assumption. Unfortunately, the academic community has not reached a consistent conclusion that what kind of theoretical model can be relied on. The main source comes from the understanding of the complexity of interfacial and size effects, which also includes several other factors, like wall flexibility, surface roughness, boundary conditions, evaporation and condensation, etc., as illustrated in Figure 4. In a recent review [7], it was pointed out that "Overall, fluids in molecular-scale confinement are largely an uncharted territory for theory".

5.1 Capillarity and wetting

As discussed earlier, an appropriate assessment of the driving force is essential to recognizing the molecular transport under confinement. For the water flow through 2D slits, an extended meniscus is supposed to locate at the capillary openings. Under this circumstance, the disjoining pressure is introduced to interpret the deviations of water flux from the expectations of the continuum transport [36]. Before taking the liquid flow through nanochannels as the research object without the entrance effect, we would check whether the evaporation or condensation is the limiting process in the entire system [45].

We can also image that the contact line exists at the mouth of nanocapillaries. From this point of view, although liquid flow in channels and droplet on substrates are two distinct kinds of solid-liquid systems, they are inextricably linked. The competition between several capillary forces determines the motion of the contact line, pinning or depinning. The underlying mechanism of capillary force balance at the contact line was investigated [54,55]. As the interface ten-

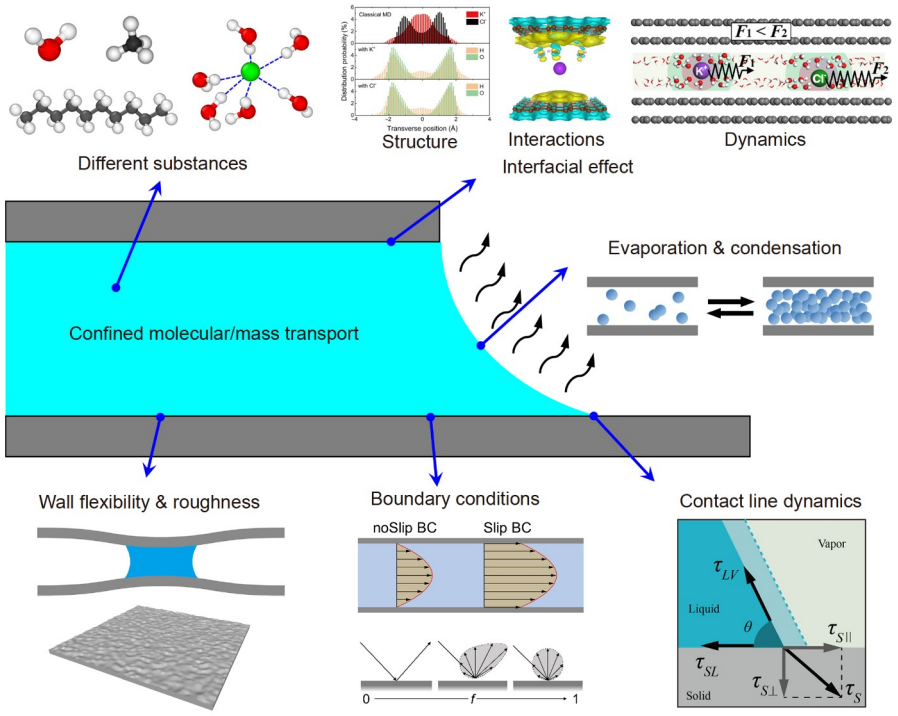

Figure 4 (Color online) Various influencing factors in confined molecular/mass transport. Two insets on the upper right corner are reprinted with permission from ref. [16]. Copyright©2019 American Chemical Society.

sion was decomposed into different terms, a novel approach to describe and quantify the capillary force on the liquid in coexistence with its vapor phase was proposed. On lyophilic surfaces with strong solid-liquid interactions, the contact angle of a nanodroplet can be smaller than 30°. The liquid-vapor and solid-liquid interfaces start to overlap and the evaluation on capillary forces in this case should be cautious [54]. For even more lyophilic surfaces, the effect of precursor film should be taken into account [56,57]. The influence of topological features on confined mass transport and wetting phenomenon also plays an important role [58,59].

5.2 Slip flow and boundary conditions

Slip boundary conditions have been a long-standing and historic controversy, especially for the nanoscale flow [60,61]. No one disputes the existence of slip, but it is still a great challenge how to describe it precisely [62]. Boundary conditions are essential for solving the governing equations. The reported values on the slip length are rather scattered in ref. [63]. There are so many influencing factors, such as solid-liquid interactions, surface roughness, the curvature effect or even the driving force [64].

For atomically smooth surfaces, like graphene, the slip length of water is generally considered to be in the range of 10-200 nm, probably much larger than the channel height [36,60]. From another aspect, there are distinctly different slip behaviors for water flow in CNTs and BN nanotubes, albeit with their similar geometries and atomically smooth interiors. The discrepancy was attributed to the different electronic properties [43]. OH^- groups resulting from the self-ionization of water molecules exhibit different adsorption behaviors on graphene and BN surfaces [65]. MD simulations have shown that even a small portion of chemical functionalization on graphene would lead to a remarkable reduction in the slip length [66].

5.3 Beyond continuum mechanics

The breakdown of continuum mechanics under extreme confinement has become a common recognition. Accordingly, there is also an urgent demand to develop new theories. For the pressure-driven water flow through channels of several nanometers in height, MD results can reproduce the parabolic velocity profiles, which agrees with the prediction from Navier-Stokes equation. Whereas, a continuum limit of 1 nm has been proposed and widely accepted [7,9]. The typical size of a water molecule can be considered to be about 2.8 Å. A channel with size below this continuum limit can only accommodate no more than 3 layers of water. In these cases, it is unrealistic to anticipate the parabolic velocity profiles from 2 or 3 water layers, not to mention the monolayer water. Kinetic models for discrete particles may probably provide an approach to solve the problem, although there is still a long way to go.

6 Concluding remarks and prospects

In this review, we summarized the latest research progresses of molecular transport under extreme confinement, mainly based on the elaborately designed nanochannels which were recently proposed. We first briefly described the fabrication procedure of the vdW assembly. Then we discussed experimental investigations and MD simulations on the transport of water, ions and gases through these slit-like nanocapillaries. Special attention was paid to the new insight from MD simulations and suggested that this issue should be considered from a wider perspective, including the contact line dynamics and boundary conditions.

Despite this, significant challenges still remain to solve this problem completely. There are several future open questions. (1) It is a great advance that the slit-like nanocapillaries can disentangle some complex factors. Yet, we are still struggling with the wall flexibility and phase change phenomena at the capillary entrance. (2) The popular water models widely employed in literature were parameterized to reproduce bulk properties. Researchers may look forward to a more powerful model which takes account of the polarization effect of water molecules and even the possible chemical interactions with the solid wall. (3) We should be cautious when dealing with some common basic concepts, such as viscosity and pressure. Below the continuum limit, they might have an unexpected impact on the establishment of theory for molecular transport under confinement.

This work was supported by the National Key Research and Development Program of China (Grant No. 2019YFA0708700), the National Natural Science Foundation of China (Grant No. 11922213), the Fundamental Research Funds for the Central Universities (Grant No. WK2480000005), and the Youth Innovation Promotion Association CAS (Grant No. 2020449). The authors express their thanks to Quan Wang for helping with the artwork in Figure 2(g).

1 Y. P. Zhao, *Physical Mechanics of Surfaces and Interfaces* (in Chinese) (Science Press, Beijing, 2012).
2 Y. P. Zhao, *Lectures on Mechanics* (in Chinese) (Science Press, Beijing, 2018).
3 T. Jacobsen, and S. Lloyd, *Sennacherib's Aqueduct at Jerwan* (University of Chicago Press, Chicago, 1935), p. 34.
4 H. Lamb, *Hydrodynamics* (Cambridge University Press, Cambridge, 1945).
5 G. Karniadakis, A. Beskok, and N. Aluru, *Microflows and Nanoflows: Fundamentals and Simulation* (Springer Science & Business Media, New York, 2005).
6 R. B. Schoch, J. Han, and P. Renaud, Rev. Mod. Phys. **80**, 839 (2008).
7 N. Kavokine, R. R. Netz, and L. Bocquet, Annu. Rev. Fluid Mech. **53**, 377 (2021), arXiv: 2011.14111.
8 L. Bocquet, Nat. Mater. **19**, 254 (2020), arXiv: 2003.00211.
9 L. Bocquet, and E. Charlaix, Chem. Soc. Rev. **39**, 1073 (2010).
10 J. N. Israelachvili, and R. M. Pashley, Nature **306**, 249 (1983).
11 S. Granick, Science **253**, 1374 (1991).
12 J. N. Israelachvili, and P. M. McGuiggan, Science **241**, 795 (1988).
13 J. A. Thomas, and A. J. H. McGaughey, Phys. Rev. Lett. **102**, 184502 (2009).
14 Q. Yuan, and Y. P. Zhao, J. Am. Chem. Soc. **131**, 6374 (2009).
15 Q. Yang, P. Z. Sun, L. Fumagalli, Y. V. Stebunov, S. J. Haigh, Z. W. Zhou, I. V. Grigorieva, F. C. Wang, and A. K. Geim, Nature **588**, 250 (2020), arXiv: 2009.11238.
16 Y. Z. Yu, J. C. Fan, A. Esfandiar, Y. B. Zhu, H. A. Wu, and F. C. Wang, J. Phys. Chem. C **123**, 1462 (2019).
17 G. Algara-Siller, O. Lehtinen, F. C. Wang, R. R. Nair, U. Kaiser, H. A. Wu, A. K. Geim, and I. V. Grigorieva, Nature **519**, 443 (2015), arXiv: 1412.7498.
18 W. Zhou, K. Yin, C. Wang, Y. Zhang, T. Xu, A. Borisevich, L. Sun, J. C. Idrobo, M. F. Chisholm, S. T. Pantelides, R. F. Klie, and A. R. Lupini, Nature **528**, E1 (2015).
19 J. Chen, G. Schusteritsch, C. J. Pickard, C. G. Salzmann, and A. Michaelides, Phys. Rev. Lett. **116**, 025501 (2016), arXiv: 1508.03743.
20 Y. B. Zhu, F. C. Wang, J. Bai, X. C. Zeng, and H. A. Wu, ACS Nano **9**, 12197 (2015).
21 J. C. Li, Y. B. Zhu, J. Xia, J. C. Fan, H. A. Wu, and F. C. Wang, J. Chem. Phys. **154**, 224508 (2021).
22 L. Fumagalli, A. Esfandiar, R. Fabregas, S. Hu, P. Ares, A. Janardanan, Q. Yang, B. Radha, T. Taniguchi, K. Watanabe, G. Gomila, K. S. Novoselov, and A. K. Geim, Science **360**, 1339 (2018), arXiv: 1806.04486.
23 D. Muñoz-Santiburcio, and D. Marx, Chem. Rev. **121**, 6293 (2021).
24 S. Sahu, and M. Zwolak, Rev. Mod. Phys. **91**, 021004 (2019), arXiv: 1809.05098.
25 J. Shen, G. Liu, Y. Han, and W. Jin, Nat. Rev. Mater. **6**, 294 (2021).
26 K. Lin, X. Huang, and Y. P. Zhao, Energy Fuels **34**, 258 (2020).
27 H. Yu, H. Y. Xu, J. C. Fan, Y. B. Zhu, F. C. Wang, and H. A. Wu, Energy Fuels **35**, 911 (2021).
28 J. H. Qian, Y. H. Li, H. A. Wu, and F. C. Wang, Carbon **180**, 85 (2021).
29 L. Sun, H. Liu, W. He, G. Li, S. Zhang, R. Zhu, X. Jin, S. Meng, and H. Jiang, Pet. Explor. Dev. **48**, 527 (2021).
30 D. Wang, Y. Tian, and L. Jiang, Small **17**, 2100788 (2021).
31 J. Zhong, M. A. Alibakhshi, Q. Xie, J. Riordon, Y. Xu, C. Duan, and D. Sinton, Acc. Chem. Res. **53**, 347 (2020).
32 R. R. Nair, H. A. Wu, P. N. Jayaram, I. V. Grigorieva, and A. K. Geim, Science **335**, 442 (2012), arXiv: 1112.3488.
33 R. K. Joshi, P. Carbone, F. C. Wang, V. G. Kravets, Y. Su, I. V. Grigorieva, H. A. Wu, A. K. Geim, and R. R. Nair, Science **343**, 752 (2014), arXiv: 1401.3134.
34 J. Abraham, K. S. Vasu, C. D. Williams, K. Gopinadhan, Y. Su, C. T. Cherian, J. Dix, E. Prestat, S. J. Haigh, I. V. Grigorieva, P. Carbone, A. K. Geim, and R. R. Nair, Nat. Nanotech. **12**, 546 (2017), arXiv: 1701.05519.
35 S. Zhao, C. Jiang, J. Fan, S. Hong, P. Mei, R. Yao, Y. Liu, S. Zhang, H. Li, H. Zhang, C. Sun, Z. Guo, P. Shao, Y. Zhu, J. Zhang, L. Guo, Y. Ma, J. Zhang, X. Feng, F. Wang, H. Wu, and B. Wang, Nat. Mater. **20**, 1551 (2021).
36 B. Radha, A. Esfandiar, F. C. Wang, A. P. Rooney, K. Gopinadhan, A. Keerthi, A. Mishchenko, A. Janardanan, P. Blake, L. Fumagalli, M. Lozada-Hidalgo, S. Garaj, S. J. Haigh, I. V. Grigorieva, H. A. Wu, and A. K. Geim, Nature **538**, 222 (2016), arXiv: 1606.09051.
37 A. Esfandiar, B. Radha, F. C. Wang, Q. Yang, S. Hu, S. Garaj, R. R. Nair, A. K. Geim, and K. Gopinadhan, Science **358**, 511 (2017), arXiv: 1709.03928.
38 A. Keerthi, A. K. Geim, A. Janardanan, A. P. Rooney, A. Esfandiar, S. Hu, S. A. Dar, I. V. Grigorieva, S. J. Haigh, F. C. Wang, and B. Radha, Nature **558**, 420 (2018), arXiv: 1805.05835.
39 K. Gopinadhan, S. Hu, A. Esfandiar, M. Lozada-Hidalgo, F. C. Wang, Q. Yang, A. V. Tyurnina, A. Keerthi, B. Radha, and A. K. Geim, Science **363**, 145 (2019), arXiv: 1811.09227.
40 A. K. Geim, and I. V. Grigorieva, Nature **499**, 419 (2013).
41 A. K. Geim, Nano Lett. **21**, 6356 (2021), arXiv: 2107.12149.
42 D. A. Bandurin, I. Torre, R. Krishna Kumar, M. Ben Shalom, A. Tomadin, A. Principi, G. H. Auton, E. Khestanova, K. S. Novoselov, I.

V. Grigorieva, L. A. Ponomarenko, A. K. Geim, and M. Polini, Science **351**, 1055 (2016), arXiv: 1509.04165.
43 E. Secchi, S. Marbach, A. Niguès, D. Stein, A. Siria, and L. Bocquet, Nature **537**, 210 (2016).
44 Y. Z. Yu, J. C. Fan, J. Xia, Y. B. Zhu, H. A. Wu, and F. C. Wang, Nanoscale **11**, 8449 (2019).
45 J. C. Fan, H. A. Wu, and F. C. Wang, Phys. Fluids **32**, 012001 (2020).
46 S. Gravelle, C. Ybert, L. Bocquet, and L. Joly, Phys. Rev. E **93**, 033123 (2016), arXiv: 1603.07918.
47 Y. H. Li, Y. Z. Yu, J. H. Qian, H. A. Wu, and F. C. Wang, Appl. Surf. Sci. **560**, 150022 (2021).
48 C. Vega, and J. L. F. Abascal, Phys. Chem. Chem. Phys. **13**, 19663 (2011).
49 H. Chan, M. J. Cherukara, B. Narayanan, T. D. Loeffler, C. Benmore, S. K. Gray, and S. K. R. S. Sankaranarayanan, Nat. Commun. **10**, 379 (2019).
50 T. D. Loeffler, H. Chan, K. Sasikumar, B. Narayanan, M. J. Cherukara, S. Gray, and S. K. R. S. Sankaranarayanan, J. Phys. Chem. C **123**, 22643 (2019).
51 H. F. Ye, J. Wang, Y. G. Zheng, H. W. Zhang, and Z. Chen, Phys. Chem. Chem. Phys. **23**, 10164 (2021).
52 Q. Miao, Q. Yuan, and Y. P. Zhao, Microfluid Nanofluid **22**, 141 (2018).
53 Q. Miao, Q. Yuan, and Y. P. Zhao, Phys. Fluids **32**, 102103 (2020).
54 J. C. Fan, J. De Coninck, H. A. Wu, and F. C. Wang, Phys. Rev. Lett. **124**, 125502 (2020).
55 J. C. Fan, J. De Coninck, H. A. Wu, and F. C. Wang, J. Colloid Interface Sci. **585**, 320 (2021).
56 Y. P. Zhao, Sci. China-Phys. Mech. Astron. **59**, 114631 (2016).
57 Q. Yuan, and Y. P. Zhao, Phys. Rev. Lett. **104**, 246101 (2010).
58 X. T. Yan, Y. K. Jin, X. M. Chen, C. Zhang, C. L. Hao, and Z. K. Wang, Sci. China-Phys. Mech. Astron. **63**, 224601 (2020).
59 J. Lou, S. L. Shi, C. Ma, C. J. Lv, and Q. S. Zheng, Sci. China-Phys. Mech. Astron. **64**, 244711 (2021).
60 F. C. Wang, and Y. P. Zhao, Soft Matter **7**, 8628 (2011).
61 L. Y. Wang, F. C. Wang, F. Q. Yang, and H. A. Wu, Sci. China-Phys. Mech. Astron. **57**, 2152 (2014).
62 Q. Xie, M. A. Alibakhshi, S. Jiao, Z. Xu, M. Hempel, J. Kong, H. G. Park, and C. Duan, Nat. Nanotech. **13**, 238 (2018).
63 S. K. Kannam, B. D. Todd, J. S. Hansen, and P. J. Daivis, J. Chem. Phys. **138**, 094701 (2013).
64 F. Wang, and Y. Zhao, Acta Mech. Solid Sin. **24**, 101 (2011).
65 B. Grosjean, C. Pean, A. Siria, L. Bocquet, R. Vuilleumier, and M. L. Bocquet, J. Phys. Chem. Lett. **7**, 4695 (2016).
66 N. Wei, X. Peng, and Z. Xu, Phys. Rev. E **89**, 012113 (2014), arXiv: 1308.5367.